

University of Groningen

Instantons and cosmologies in string theory

Collinucci, Giulio

IMPORTANT NOTE: You are advised to consult the publisher's version (publisher's PDF) if you wish to cite from it. Please check the document version below.

Document Version

Publisher's PDF, also known as Version of record

Publication date:

2005

[Link to publication in University of Groningen/UMCG research database](#)

Citation for published version (APA):

Collinucci, G. (2005). *Instantons and cosmologies in string theory*. s.n.

Copyright

Other than for strictly personal use, it is not permitted to download or to forward/distribute the text or part of it without the consent of the author(s) and/or copyright holder(s), unless the work is under an open content license (like Creative Commons).

The publication may also be distributed here under the terms of Article 25fa of the Dutch Copyright Act, indicated by the "Taverne" license. More information can be found on the University of Groningen website: <https://www.rug.nl/library/open-access/self-archiving-pure/taverne-amendment>.

Take-down policy

If you believe that this document breaches copyright please contact us providing details, and we will remove access to the work immediately and investigate your claim.

Downloaded from the University of Groningen/UMCG research database (Pure): <http://www.rug.nl/research/portal>. For technical reasons the number of authors shown on this cover page is limited to 10 maximum.

Chapter 6

Scalar Cosmologies II: A not so simple case

6.1 Introduction

In chapter 5, we studied scalar cosmology models, specializing in the single exponential potential case. We wrote down the field equations in the form of an autonomous system and studied its critical points and its interpolating solutions. However, the assumption of a single exponential in the potential lead to a great simplification, namely the amount of scalar fields was effectively reduced to two. In this chapter, we will drop this simplifying assumption and look at multi-exponential potentials.

The understanding of multi-exponential potentials has gradually evolved over the years. In the early days, the single exponential was studied in the context of inflation, where it was discovered that this potential allowed for a power-law solution [104]. Later on, the effect of adding exponential terms, each carrying a different scalar, was studied. This model is called “assisted inflation” [108]. The outcome is that the scalars ‘assist’ each other in the sense that each term contributes in the same way to the power-law behaviour of the scale factor and all the contributions are added. Later on, the effect of a cross-coupling between scalars was searched for, resulting in a model called “generalized assisted inflation” [122]. It was shown that these multi-exponential potentials also allowed for power-law solutions. However, the understanding of multi-exponential potentials wasn’t complete. The class of potentials described in [122] does not cover all possible multi-exponential potentials. There is a strong restriction on the scalar couplings in that model, such that it only allows for power-law solutions. In other words, the potentials do not have any extrema. However, nowadays, a considerable amount of models that are inspired by string theory seem to be multi-exponentials with extrema (which allow for de Sitter solutions). Hence, they do not fall in the class of generalized assisted inflation.

The goal of this chapter is to study the most general multi-exponential potential. This is done using the elegant formalism of autonomous dynamical systems. We will construct all possible power-law and de Sitter solutions by finding the critical points to which they correspond in this formalism. We point out that this will uncover many new power-law and de Sitter solu-

tions corresponding to so-called non-proper critical points that cannot be found in the case of generalized assisted inflation. To illustrate this, we will consider the special cases of double and triple exponential potentials with one or two scalars. For certain values of the scalar couplings, these can arise from M-theory, and their interpolating solutions correspond to the reduction of S-branes [117] and so-called exotic S-branes [95], respectively. For the exotic S-branes we derive the phases of accelerated expansion and find special cases where the number of such phases can be arbitrarily high. This can be useful for solving the cosmological coincidence problem, since oscillating dark energy could explain why we see a recent take over of dark energy in our present universe. It would simply be an event that occurs many times during the evolution of the universe.

The chapter is based on a collaboration with M. Nielsen and T. Van Riet, entitled *Scalar cosmology with multi-exponential potentials* [128]. It is organized as follows: in section 2, we present the system consisting of gravity and scalars with a potential. In section 3, we perform the general analysis of critical points. In section 4, we consider the special cases of double exponentials. In section 5, we present cases that can be obtained from the reduction over a three-dimensional group manifold. Finally, we end with a discussion of our results in section 6.

6.2 Scalar gravity with multi-exponential potentials

We consider 4-dimensional spatially flat FLRW gravity with N scalars ϕ_I which only depend on (cosmic) time τ . The scalars have a potential which is of the most general exponential form:

$$V(\vec{\phi}) = \sum_{i=1}^m \Lambda_i e^{-\vec{\alpha}_i \cdot \vec{\phi}}. \quad (6.1)$$

Thus, the scalar potential is characterized by m vectors $\vec{\alpha}_i$ and m constants Λ_i which can have positive or negative signs. The $\vec{\alpha}_i$ vectors form an $m \times N$ matrix α_{iI} , where the indices $i = 1, \dots, m$ parametrize the exponential terms in the potential and the indices $I = 1, \dots, N$ parametrize the different scalars. The Lagrangian for the system then reads¹:

$$\mathcal{L} = \sqrt{-g} \left(R - \frac{1}{2} (\partial\vec{\phi})^2 - V(\vec{\phi}) \right). \quad (6.2)$$

The equations of motion derived from the Lagrangian are

$$\begin{aligned} \ddot{\phi}_I + 3H\dot{\phi}_I + \frac{\partial V}{\partial \phi_I} &= 0, \\ H^2 &= \frac{1}{12} (\dot{\vec{\phi}} \cdot \dot{\vec{\phi}}) + \frac{1}{6} V, \\ \dot{H} &= -\frac{1}{4} (\dot{\vec{\phi}} \cdot \dot{\vec{\phi}}), \end{aligned} \quad (6.3)$$

where the dot is differentiation w.r.t. cosmic time. We refer to the equations as the scalar equations, the Friedmann equation and the acceleration equation, respectively. The Hubble constant H is defined as $H = \dot{a}/a$ where $a(\tau)$ is the scale factor appearing in the flat FLRW metric:

$$ds^2 = -d\tau^2 + a(\tau)^2 dx_3^2. \quad (6.4)$$

¹We use the convention for the metric with mostly plus signature.

There are $N + 1$ degrees of freedom, namely, the scale factor and the N scalars (and accordingly only $N + 1$ equations of motion are independent). For example, the acceleration equation can be obtained from the Friedmann equation and the scalar equations). There exist 2 types of solutions:

- **Critical points:** These solutions correspond to stationary solutions defined in terms of certain dimensionless variables, which will be introduced in the next section. The critical points can be obtained explicitly and they correspond to power-law solutions ($a(\tau) \sim \tau^p$) or de Sitter solutions² ($a(\tau) \sim e^\tau$). The solutions can be attractors, repellers or saddle points. In the former two cases they correspond to the asymptotic behaviour of more general solutions, whereas a saddle point just corresponds to an intermediate regime.
- **Interpolating solutions:** These are the non-stationary solutions and in general they will interpolate between the critical points. Often they cannot be found explicitly, but a numerical analysis can reveal most of their properties.

6.3 The critical points

Critical points (also known as fixed points or equilibrium points) are solutions of differential equations in the context of autonomous dynamical systems. An autonomous system is defined as a system described by n variables, say \vec{z} , that depend on one variable t , whose dynamical equations are of the form:

$$\frac{d\vec{z}}{dt} = \vec{f}(\vec{z}), \quad (6.5)$$

where $\vec{f}: \mathbb{R}^n \rightarrow \mathbb{R}^n$ is interpreted as a vector field on \mathbb{R}^n . A key feature of autonomous systems is the absence of the independent variable t on the right-hand-side of the dynamical equation (6.5). Solutions for $\vec{z}(t)$ are then integral curves to the vector field \vec{f} ; i.e. \vec{f} is everywhere tangent to all possible curves $\vec{z}(t)$. The critical points of an autonomous system are defined as those points \vec{z}_0 obeying $\vec{f}(\vec{z}_0) = 0$. These points are always exact constant solutions since $d\vec{z}_0(t)/dt = 0$. The interesting property about these systems is that the critical points are often the end points (and initial points) of the orbits and therefore describe the asymptotic behaviour. If the solutions interpolate between critical points, they can be divided into two classes:

- **Heteroclinic orbit:** This is an orbit connecting two different critical points.
- **Homoclinic orbit:** This is an orbit connecting a critical point to itself.

Most of the examples we have found are of the first type and we will focus on those. More on the theory of dynamical systems in cosmology can be found in [129, 130].

An useful property of multi-scalar cosmology with exponential potentials is that they allow for a description in terms of variables that make the system autonomous [104, 106, 107, 110]. With an arbitrary multi-exponential potential, the variables are defined as follows:

$$x_I = \frac{\dot{\phi}_I}{\sqrt{12}H}, \quad y_i = \sqrt{\frac{\Lambda_i e^{-\vec{\alpha}_i \cdot \vec{\phi}}}{6H^2}}. \quad (6.6)$$

²Anti-de Sitter solutions are not possible since a flat FLRW metric doesn't support them.

In this notation, there are $N + m$ variables. Note that y_i will be imaginary when $\Lambda_i < 0$, but this is not a problem since only y_i^2 appears in the equations of motion. Rewriting the equations of motion with these variables yields

$$\frac{\dot{x}_I}{H} = -3y^2 x_I + \sqrt{3} \sum_{i=1}^m \alpha_{iI} y_i^2, \quad (6.7)$$

$$x^2 + y^2 = 1, \quad (6.8)$$

$$\frac{\dot{H}}{H^2} = -3x^2, \quad (6.9)$$

where we have used the shorthand notation $x^2 = \sum_{I=1}^N x_I^2$ and $y^2 = \sum_{i=1}^m y_i^2$. An interesting consequence of the choice of variables is that the Friedmann equation (6.8) becomes the defining equation of an $(N + m - 1)$ -sphere for $\Lambda_i > 0$ (otherwise it will be a generalized hyperboloid). Furthermore, from the acceleration equation, the condition for accelerated expansion translates into the following simple constraint:

$$\ddot{a} > 0 \quad \Leftrightarrow \quad x^2 < \frac{1}{3}. \quad (6.10)$$

The above condition allows us to visualize the region of acceleration for the specific examples in section 4 and 5.

It turns out that we also need the derivatives of the y -variables:

$$\frac{\dot{y}_i}{H} = \sqrt{3} (\sqrt{3} x^2 - \vec{\alpha}_i \cdot \vec{x}) y_i. \quad (6.11)$$

We can also use $\ln(a)$ as evolution parameter³ instead of cosmic time, which simplifies the equations since H drops out in the scalar equations of motion and the equations for \dot{y}_i , giving

$$\boxed{x'_I = -3y^2 x_I + \sqrt{3} \sum_{i=1}^m \alpha_{iI} y_i^2, \quad y'_i = \sqrt{3} (\sqrt{3} x^2 - \vec{\alpha}_i \cdot \vec{x}) y_i,} \quad (6.12)$$

where the prime indicates differentiation w.r.t. $\ln(a)$. The above is clearly of the form (6.5), and the critical points can therefore be calculated as $x'_I = y'_i = 0$ (or equivalently as $\dot{x}_I = \dot{y}_i = 0$). It is easy to prove that the system will obey the Friedmann constraint (6.8) at all times as long as it does so initially. Hence, if we impose (6.8) on the initial conditions, then (6.12) contains all the information about the subsequent evolution.

Integrating the acceleration equation (6.9) for a critical point yields power-law solutions if $x^2 \neq 0$

$$a(\tau) \sim \tau^p, \quad p = \frac{1}{3x^2}. \quad (6.13)$$

If on the other hand, if $x^2 = 0$, then the critical point is an extremum of the potential with a de Sitter expansion

$$a(\tau) \sim \exp\left(\sqrt{\frac{1}{6}V(\phi_c)} \tau\right). \quad (6.14)$$

³However, one must be careful if the scale factor is not strictly monotonic.

The equations (6.12) determining the critical points are

$$(\sqrt{3} x^2 - \vec{\alpha}_i \cdot \vec{x}) y_i = 0, \quad (6.15)$$

$$-3y^2 x_I + \sqrt{3} \sum_{i=1}^m \alpha_{iI} y_i^2 = 0. \quad (6.16)$$

There are two different kinds of critical points:

- Proper solutions: $\nexists i : y_i = 0$,
- Non-proper solutions: $\exists i : y_i = 0$.

We can single out special non-proper solutions, which always exist, namely, the case where all y 's vanish. From the Friedmann equation it follows that these solutions have $x^2 = 1$ and for this reason we refer to them as “the equator”. The solutions with some y 's vanishing have infinite scalars and therefore, are not proper solutions of the equations of motion. They are, however, very important, since they correspond to the asymptotic behaviour of interpolating solutions. From this classification, we see that there are a maximum of 2^m types of critical point solutions [110]. Below we will give these solutions for the most general exponential potential by analysing (6.15) and (6.16).

The rank R of the matrix α_{iI} , i.e. the number of independent $\vec{\alpha}_i$ -vectors, plays a central role in this discussion. In fact, the discussion of the general potential naturally splits up into two cases: $R = m$ and $R < m$.

The rank R gives the effective number of scalars appearing in the potential, corresponding to the part of the scalar space that is projected on the $\vec{\alpha}_i$ -vectors. It is therefore always possible to perform a field redefinition, such that only R scalars appear in the potential. The part of the scalar space perpendicular to the $\vec{\alpha}_i$ -vectors only appears in the kinetic term of the Lagrangian and is $(N - R)$ -dimensional. Therefore, these scalars decouple from the rest. All systems with $N > R$ have decoupled scalars and this is necessarily the case when $N > m$. Systems with $N \leq m$ only have decoupled scalars if the vectors $\vec{\alpha}_i$ are linearly dependent in such a way that $N > R$.

The field redefinition yielding R scalars in the potential can be performed by an $SO(N)$ rotation (which leaves the kinetic term invariant) such that $\vec{\phi}$ changes into $\vec{\phi}'$ and $\alpha'_{iR+1} = \alpha'_{iR+2} = \dots = \alpha'_{iN} = 0$ for all i . We then notice from (6.16) that, for critical points, all x 's corresponding to decoupled scalars are zero, $x_{R+1} = x_{R+2} = \dots = x_N = 0$. Therefore, in the rest of this section, the indices I now run from 1 to R . In the case $R = m$, this makes α_{iI} a square matrix.

We have seen that the discussion of the system can be split up into two cases, depending on the rank of α_{iI} . Alternatively, we can formulate this in terms of the following matrix, which is quadratic in the α 's

$$A_{ij} = \vec{\alpha}_i \cdot \vec{\alpha}_j. \quad (6.17)$$

The separation of the general exponential potential into two classes can then be characterized by the determinant of A :

$$\begin{aligned} R = m : & \quad \det(A) \neq 0, \\ R < m : & \quad \det(A) = 0. \end{aligned} \quad (6.18)$$

The first class corresponds to an invertible A -matrix and this is exactly what is termed generalized assisted inflation [122]; whereas the second class, to our knowledge, has not been treated in generality in the literature.

We will extend the existing results by also treating the case of non-invertible A in generality and providing the non proper critical points of both classes. Special examples can be obtained by performing compactifications over certain three-dimensional unimodular group manifolds corresponding to class A in the Bianchi classification, see e.g. [95].

There is a subtlety about the description in terms of the (x_I, y_i) -variables, namely if $R < m$ then the y -variables are not necessarily independent. We will comment on this in section 3.2.

6.3.1 The $R = m$ case

This case has the simplifying feature that $\dot{x}_I = 0$ implies $\dot{y}_i = 0$. This can be seen in the following way: first we differentiate (6.7) and use $\dot{x}_I = d(y^2)/d\tau = 0$. Multiplying with α_{jI} and summing over I we get $\sum_j (A_{ij}) d(y_j^2)/d\tau = 0$, and since $\det(A) \neq 0$ we know that the only solution is $d(y_i^2)/d\tau = 0$.

We will now solve for the critical points:

- Proper critical points:

From (6.15) and (6.16) we get:

$$\sum_i (A_{ij}) y_i^2 = 3y^2 x^2 e_j, \quad (6.19)$$

where e_j is an m -dimensional vector with all components equal to 1. Inverting this relation and using (6.16) yields the values of y_i and x_I for the proper critical point

$$y_i^2 = \frac{3p-1}{3p^2} \sum_{j=1}^m (A^{-1})_{ij}, \quad x_I = \frac{\sqrt{3}p}{3p-1} \sum_i \alpha_{iI} y_i^2, \quad (6.20)$$

where p is the exponent given in (6.13). The result for x_I can also be given in the rotated basis where α_{iI} is a square matrix

$$x_I = \frac{1}{\sqrt{3}p} \sum_{i=1}^m (\alpha^{-1})_{iI}. \quad (6.21)$$

Note that by construction, the A_{ij} -matrix (6.17) is $SO(N)$ -invariant and accordingly, all quantities containing only this matrix can be calculated in any basis. We notice from our formula above that there is a unique proper critical point. However, it only exists when y_i^2 , as determined from (6.20), has the same sign as Λ_i , which serves as a consistency check of definition (6.6). Thus, this critical point only exists for certain values of the α -vectors.

Using (6.13), we get the exponent for the power-law that reproduces the result found in [122, 131]:

$$p = \sum_{i,j=1}^m (A^{-1})_{ij}. \quad (6.22)$$

By integration we can go back to the ϕ_I, H variables where the solution becomes:

$$H = \frac{p}{\tau}, \quad \phi_I = \sqrt{12} p x_I \ln(\tau) + c_I, \quad y_i^2 = \frac{k_i}{\tau^2}, \quad (6.23)$$

where c_I and k_i are integration constants. In fact, in [103, 122], (6.23) was used as an Ansatz to find power-law solutions.

- **Non-proper critical points:**

These correspond to some y 's being equal to zero. Parametrising the subset of nonzero y 's with the indices a, b, c, \dots , the equations become:

$$\sqrt{3}x^2 - \vec{\alpha}_a \cdot \vec{x} = 0, \quad \sum_a \alpha_{Ia}(y_a)^2 - (1 - x^2)\sqrt{3}x_I = 0, \quad (6.24)$$

from which we deduce:

$$\sum_b (A_{ab})y_b^2 = 3y^2 x^2 e_a. \quad (6.25)$$

The $\vec{\alpha}_a$ -vectors are of course also linearly independent and accordingly, the sub-matrix A_{ab} has non-zero determinant and is therefore invertible. Inverting relation (6.25) and using (6.16), we find a unique solution

$$y_a^2 = \frac{3p-1}{3p^2} \sum_b (A^{-1})_{ab}, \quad x_I = \frac{\sqrt{3}p}{3p-1} \sum_a \alpha_{aI} y_a^2. \quad (6.26)$$

The power-law is again given by (6.22) but now with the inverse of the sub-matrix A_{ab} . Just as for the proper solution, the above is only well-defined when y_a^2 has the same sign as Λ_a . Note that all the above formulae for the non-proper critical points are similar to those for the proper ones. This is due to the fact that vanishing y 's just yield a truncated potential.

Note that since the solution for the proper critical point is unique and has power-law behaviour for the scale factor, there are no de Sitter solutions. This can also be seen from (6.19). Since A has maximal rank, this matrix only has the trivial nullspace, i.e. $y_i = 0$, which is not consistent with the Friedmann equation, since $x = 0$ for the de Sitter solutions. We can conclude that potentials with linearly independent $\vec{\alpha}_i$ -vectors generically have power-law solutions and no de Sitter solutions. This conclusion was also reached in [132] where special cases were considered.

The special case where α_{iI} is diagonalisable by an $SO(N)$ -rotation is equivalent to the case where just one scalar appears in each exponential, thus yielding the model which has been called assisted inflation [108].

6.3.2 The $R < m$ case

Since $\det(A) = 0$ we will have to use another approach to determine the critical points. And the $R < m$ case will also be more difficult to treat in full generality because the y 's are not necessarily independent.

The number of independent y 's is always smaller than or equal to $R + 1$, as we will now illustrate. After possible field redefinitions, the y -coordinates are given in terms of $R + 1$ fields, namely the scalars and the Hubble parameter. Therefore, among the m coordinates, at most $R + 1$ are independent, e.g. y_1, \dots, y_{R+1} . This leaves us with $m - R - 1$ relations for the rest of the y 's. From the definitions of the y 's, we can express ϕ_I and H in terms of the first $R + 1$ y 's

$$e^{\phi_I} = \prod_{i=1}^R \left(\frac{y_i^2 \Lambda_{i+1}}{y_{i+1}^2 \Lambda_i} \right)^{(\beta^{-1})_{Ii}}, \quad H = \frac{\Lambda_{R+1}}{6} e^{-\vec{\alpha}_{R+1} \cdot \vec{\phi}} y_{R+1}^{-2}, \quad (6.27)$$

where the following square matrix has been defined

$$\beta_{iJ} = \alpha_{i+1,J} - \alpha_{iJ}, \quad i, J \in \{1, \dots, R\}. \quad (6.28)$$

We can then express the remaining y 's in terms of the first $R + 1$ as follows

$$y_i^2 = y_{R+1}^2 \frac{\Lambda_i}{\Lambda_{R+1}} \frac{\prod_{j,K=1}^R \left(\frac{y_j^2 \Lambda_{j+1}}{y_{j+1}^2 \Lambda_j} \right)^{\alpha_{iK} (\beta^{-1})_{Kj}}}{\prod_{l,M=1}^R \left(\frac{y_l^2 \Lambda_{l+1}}{y_{l+1}^2 \Lambda_l} \right)^{\alpha_{R+1,M} (\beta^{-1})_{Ml}}}, \quad i = R + 2, \dots, m. \quad (6.29)$$

Thus, the maximal number of independent y 's is $R + 1$. It is possible to prove that the dynamical system (6.12) will obey the above relations for the y_i 's at all times if it do so initially. So again we can use (6.12) as equations that govern the whole system, as long as we pick our initial conditions consistently. With this in mind we will look for critical points.

Until now we have denoted the row vectors of the α -matrix with $\vec{\alpha}_i$ and A_{ij} was defined as the matrix with the inner products of these row vectors as entries: $A_{ij} = \vec{\alpha}_i \cdot \vec{\alpha}_j$. In this section we will also need the column vectors which we will denote by $\vec{\alpha}_I$ and we will need to define the following matrix

$$B_{IJ} = \vec{\alpha}_I \cdot \vec{\alpha}_J. \quad (6.30)$$

The R column vectors $\vec{\alpha}_I$ are all linearly independent because the rank of α equals R and, consequently, B is invertible (remember that I now runs from 1 to R). It is this property that we will use to find the solutions.

- **Proper power-law critical points:**

Looking for the solution(s), with $y_i \neq 0$, we find from (6.15)

$$\sum_{I=1}^R B_{IJ} x_I = \sqrt{3} x^2 F_J, \quad (6.31)$$

where $F_J = \sum_{i=1}^m \alpha_{iJ}$. Thus, we can solve for x_I :

$$x_I = \frac{1}{\sqrt{3} p} \sum_{J=1}^R (B^{-1})_{IJ} F_J. \quad (6.32)$$

Hence we find the extension of the power-law formula to the case where $R < m$:

$$p = |B^{-1} \cdot \vec{F}|^2. \quad (6.33)$$

One can prove that this formula reduces to (6.22) if $R = m$. Since the rank of α_{ij} is R , it is enough to use R independent equations among the m equations of (6.15) to obtain x_I . This result, of course, has to be consistent with the remaining $m - R$ equations, and this puts strong restrictions on the allowed dilaton couplings as we will now show. Let $\{\vec{\alpha}_a\}_{a=1}^R$ be linearly independent. It is possible to solve (6.15) simultaneously for these vectors. The rest of the vectors can be written as linear combinations and are only guaranteed to solve (6.15) if the linear combinations are convex ⁴

$$\vec{\alpha}_i = \sum_{a=1}^R c_{ia} \vec{\alpha}_a, \quad \sum_{a=1}^R c_{ia} = 1, \quad i = R + 1, \dots, m. \quad (6.34)$$

We will give a specific example with an M-theory origin, where this is realized. A special case is $R = 1$, where after field redefinitions only one scalar appears in the potential. In this case, the above solution will never exist, since (6.15) becomes m equations with one variable (or equivalently, the requirement of convexity here would imply $m = 1$, which is not the case under consideration).

An important difference between this and the previous case is the question of the uniqueness of the solution. We cannot obtain the y -values with this procedure, and in particular we cannot determine whether they are unique. In fact, it is easy to give an example where they are not: when at least one $\Lambda_i < 0$, we have the following possibility, since A has a non-trivial kernel

$$\begin{aligned} y^2 &= 0, & y_i^2 &\in \text{Ker}(A), \\ x^2 &= 1, & \vec{\alpha}_i \cdot \vec{x} &= \sqrt{3}, \quad \text{for } y_i \neq 0. \end{aligned} \quad (6.35)$$

In particular, this includes a proper critical point of the form (6.32) when all $y_i \neq 0$ and where furthermore

$$|B^{-1} \cdot \vec{F}|^2 = \frac{1}{3}. \quad (6.36)$$

- **De Sitter solutions:**

We have seen in the previous subsection, that de Sitter solutions do not exist for $R = m$, because the matrix A has a trivial kernel. In the present case, since A has a non-trivial kernel, making a de Sitter solution is possible, we have the following:

$$x = 0, \quad y^2 = 1, \quad y_i^2 \in \text{Ker}(A). \quad (6.37)$$

Again, this solution is only well-defined when y_i^2 has the same sign as Λ_i . We can conclude that potentials with $R < m$ show the opposite behaviour of $R = m$ potentials. Here, (proper) power-law solutions are rare (only possible for certain couplings (6.34)), whereas de Sitter solutions are quite generic. Again, a similar observation was made in [132], but for specific couplings (which did not allow power-law behaviour).

⁴Of course, there are many ways to number the vectors; it suffices to find one that obeys these relations.

- **Non-proper critical points:**

Looking for these solutions, we again put a subset of the y 's to zero. This corresponds to some terms in the potential being absent. Therefore, we can analyse the new system as before but with a “truncated” potential. A subtlety appears whenever $R < m$, namely the y 's are dependent on each other, and therefore only certain subsets of the y 's can be zero simultaneously.

The findings of this section are summarized in the table below. The asterisk in the lower left corner stands for a truncated system, which can belong to either of the two cases ($R < m$ or $R = m$).

	$R < m, \quad \det(A) = 0$	$R = m, \quad \det(A) \neq 0$
Proper	Power-law (convex combinations)	Power-law
	de Sitter	No de Sitter
Non-proper	*	Power-law
		No de Sitter

Table 6.1: *The critical points for multi-exponential potentials.*

As mentioned before, the critical points give rise to the asymptotic behaviour of the general solutions. By performing stability analysis it is possible to determine the nature of the critical points, i.e. whether they are attractors, repellers, or saddle points. This can be done by linearizing the system around the critical points, $\dot{\vec{x}} = \mathbf{M} \cdot \vec{x}$, and determining the eigenvalues of the matrix \mathbf{M} . If the real part of all eigenvalues is negative, the critical point is an attractor; if the real part of all eigenvalues is positive, the critical point is a repeller; and in the mixed case it is a saddle point. It is easy to perform the stability analysis in the simple cases considered in the following sections, and the result is confirmed by the interpolating solutions, which are calculated numerically.

6.4 Double and triple exponential potentials

In this section we will consider some specific examples of double and triple exponential potentials with one or two scalars, i.e. $m = 2, 3$ and $N = 1, 2$. These examples serve as an illustration of the formal framework in the previous section.

As mentioned before, the critical points reveal the asymptotic behaviour of more general solutions. In some cases it has been possible to obtain these solutions exactly. For single exponential potentials, this was done for arbitrary dilaton couplings and the result can be pictured as straight lines in the space defined by the x 's [95]. For double exponential potentials, exact solutions were obtained for special values of the dilaton couplings, corresponding to the reduction of S-brane solutions to 4D, see e.g. [91, 92, 94] and references therein. Ideally, we would like to obtain exact results for the general case. However, this is a highly non-trivial task, and we

therefore turn to numerical methods, which can still show the qualitative behaviour of the solutions. To this end, it is convenient to use $\ln(a)$ as a time parameter. For an eternally expanding universe where a increases from 0 to ∞ , our time coordinate ranges from $-\infty$ to ∞ .

In general, an S-brane can be obtained as a time-dependent solution to the following system containing gravity, an antisymmetric tensor, and possibly a dilaton:

$$S = \int d^{4+d}x \sqrt{-\hat{g}} \left(\hat{R} - \frac{1}{2} (\partial\hat{\phi})^2 - \frac{1}{2d!} e^{-b\hat{\phi}} \hat{F}_d^2 \right), \quad (6.38)$$

where the hats indicate that the fields live in $4 + d$ dimensions and where the dilaton coupling for maximal supergravities is given by

$$b = \sqrt{\frac{14 - 2d}{d + 2}}. \quad (6.39)$$

Reducing over a d -dimensional maximally symmetric space with curvature k and flux f yields the following potential [133]

$$V(\phi, \varphi) = f^2 e^{-b\phi-3\sqrt{\frac{d}{d+2}}\varphi} - k e^{-\sqrt{\frac{d+2}{d}}\varphi}, \quad (6.40)$$

where φ is the Kaluza-Klein scalar. S2-brane solutions have been found in six to eleven dimensions, corresponding to $d = 2, \dots, 7$. In five dimensions, an S2-brane has a 1-form field strength. The corresponding four-dimensional cosmological solution with single exponential potential was found in [95]. As explained in that paper, a general twisted reduction leads to triple exponential potentials, which could have corresponding exotic S-brane solutions in five dimensions.

6.4.1 Double exponential potentials, one scalar

The simplest case is $m = 2$ and $N = 1$. The corresponding potential is described in terms of two dilaton couplings α_1 and α_2 . We can always choose e.g. α_1 to be positive and in this example we will start by considering positive Λ_i . Since $R = 1$, we have 2 independent y 's. The Friedmann equation defines a 2-sphere, but the allowed solutions can only lie on the part corresponding to non-negative y 's. Using the machinery from the previous section, we find the following critical points

$$\begin{aligned} (i) \quad & y_1 = y_2 = 0, \quad x^2 = 1, \\ (ii) \quad & y_1 = \sqrt{1 - \frac{\alpha_1^2}{3}}, \quad y_2 = 0, \quad x = \frac{\alpha_1}{\sqrt{3}}, \quad \text{for } \alpha_1^2 < 3, \\ (iii) \quad & y_1 = 0, \quad y_2 = \sqrt{1 - \frac{\alpha_2^2}{3}}, \quad x = \frac{\alpha_2}{\sqrt{3}}, \quad \text{for } \alpha_2^2 < 3, \\ (iv) \quad & y_1 = (1 - \frac{\alpha_1}{\alpha_2})^{-1/2}, \quad y_2 = (1 - \frac{\alpha_2}{\alpha_1})^{-1/2}, \quad x = 0, \quad \text{for } \alpha_2 < 0. \end{aligned} \quad (6.41)$$

The first, (i) corresponds to the ‘‘equatorial’’ points $x = \pm 1$. In an (y_1, y_2, x) -plot these become the North and South Pole. The next two, (ii) and (iii), are the non-proper critical points. The

last one, (iv), is the proper solution, which only exists for $\alpha_2 < 0$ and corresponds to a de Sitter solution. The stability of the different points is best illustrated by considering the different possible cases⁵.

- $\alpha_1, \alpha_2 > \sqrt{3}$: Only the North and South Pole are critical points; the former is attracting and the latter repelling. Any interpolating solution will be a curve between them, and these can be found numerically. An example is illustrated in figure 6.1(a).
- $\alpha_1 < \alpha_2 < \sqrt{3}$: The critical points (i)-(iii) exist. The poles are repellers and (iii) is attracting.
- $\alpha_1 < \sqrt{3}, \alpha_2 < -\sqrt{3}$: Apart from the poles, we have the two critical points, corresponding to (iii) and (iv) in (6.41). The North Pole is repelling and the de Sitter solution is attracting; this is shown in figure 6.1(b).

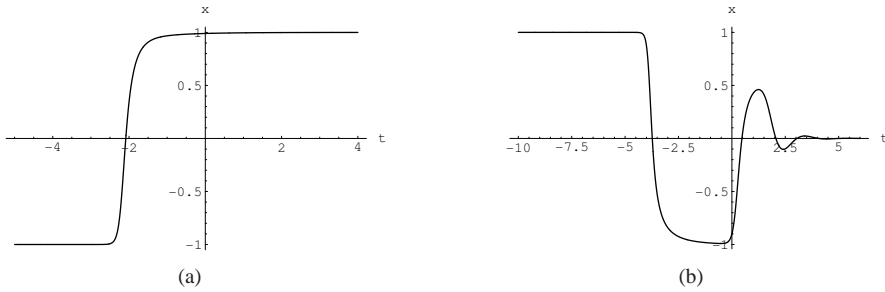


Figure 6.1: Plot (a) shows $x(t)$ in the case $(\alpha_1, \alpha_2) = (3, 2)$, where the solution interpolates between the North and South Pole. Plot (b) is for the case $(\alpha_1, \alpha_2) = (1, -2)$, yielding a solution interpolating between the North Pole and a de Sitter solution.

- $\alpha_1 > \sqrt{3}, -\sqrt{3} < \alpha_2 < 0$: This is similar to the previous case, except that the critical point (iii) is interchanged with (ii), and the early asymptotics will be the South Pole.
- $\alpha_1 > \sqrt{3}, 0 < \alpha_2 < \sqrt{3}$: In addition to the North and South Pole, there is the non-proper critical point (ii), which is an attractor. The South Pole is repelling. An interpolating solution is shown in figure 6.2(a).
- $\alpha_1 > \sqrt{3}, \alpha_2 < -\sqrt{3}$: The critical points are the poles and the de Sitter solution, and the latter is an attractor. It turns out that the poles are saddle points; hence, they do not give rise to the early asymptotics of the solution. Instead, this will be an infinite cycle, moving closer and closer to the boundary of the space (given by $y_1 = 0$ or $y_2 = 0$), as time goes to minus infinity. This is illustrated in figure 6.2(b).
- $\alpha_1 < \sqrt{3}, -\sqrt{3} < \alpha_2 < 0$: The late-time asymptotics are similar to those of the previous case. The early-time asymptotics are different due to the fact that all the critical points (i)-(iv) are realized. Both of the poles will be repelling, and depending on initial conditions, either of these can give rise to the early-time asymptotics.

⁵If we do not explicitly classify the stability of a critical point, it will be a saddle point.

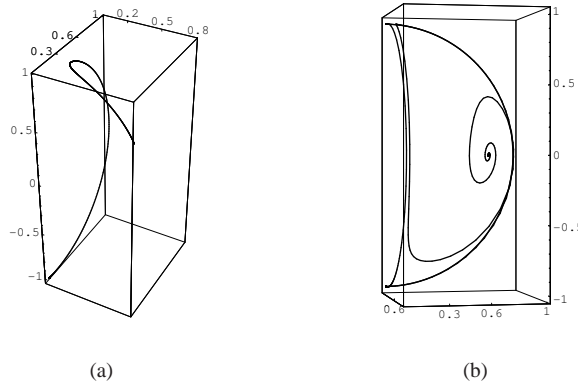


Figure 6.2: The figure shows (y_1, y_2, x) -plots for two cases. Figure (a) with $(\alpha_1, \alpha_2) = (2, 1)$, shows a solution interpolating between the South Pole and the critical point (ii). Plot (b), with $(\alpha_1, \alpha_2) = (3, -2)$ shows a solution spiralling towards the de Sitter point.

For all the cases above, the solutions enter a phase of acceleration when $x^2 < 1/3$. The cases with $|\alpha_1|, |\alpha_2| > 1$ give rise to one period of transient acceleration, otherwise the solution will end up in a phase of eternal acceleration, which, as mentioned before, is an asymptotic de Sitter phase when $\alpha_2 < 0$. In the case $\alpha_1 > \sqrt{3}, \alpha_2 < -\sqrt{3}$ the phase of late-time acceleration is preceded by an infinite cycle, alternating between acceleration and deceleration.

The case with $\Lambda_2 < 0$ can be analysed in a similar way, but the interpolating solutions will now be given by curves on a hyperboloid. The critical point (iii) will only exist for $\alpha_2^2 > 3$, since this yields $y_2^2 < 0$. By the same token, the de Sitter critical point (iv) only exists for $\alpha_2 > \alpha_1 > 0$.

The S-brane case corresponding to $\hat{\phi} = 0$ in (6.38), gives the following dilaton couplings

$$\alpha_1 = 3 \sqrt{\frac{d}{d+2}}, \quad \alpha_2 = \sqrt{\frac{d+2}{d}}. \quad (6.42)$$

This system, which can be obtained from eleven dimensions where it will give rise to SM2-brane solutions, was analysed in [96], where curvature of the external space is also included. One can show that only the critical points (i) and (iii) exist for $\Lambda_2 > 0$; and (i) and (ii) exist for $\Lambda_2 < 0$, with the latter being attracting. However, in the latter case, we also have a de Sitter critical point, which is not an attractor.

6.4.2 Double exponential potential, two scalars

Let us now study the case with double exponential potentials and two scalars, i.e. $m = 2$ and $N = 2$. Considering the two α -vectors to be independent, we get $R = 2$. The critical points can be obtained as a special case of the general analysis from the previous section and consist of the equator, $x^2 = 1, y_i = 0$; the proper critical point, $y_i \neq 0$; and two non-proper critical points with $y_i = 0, y_j \neq 0, i \neq j$.

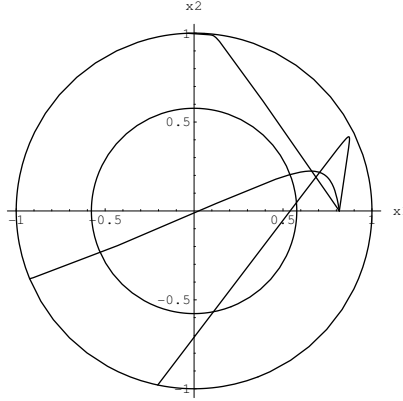


Figure 6.3: Three interpolating solutions, corresponding to S2-branes reduced to four dimensions, projected on the (x_1, x_2) -plane. The inner circle is the boundary of the accelerating region.

Specialising to the reduction of S-branes, we get the following dilaton couplings:

$$\vec{\alpha}_1 = \left(3 \sqrt{\frac{d}{d+2}}, \sqrt{\frac{14-2d}{d+2}} \right), \quad \vec{\alpha}_2 = \left(\sqrt{\frac{d+2}{d}}, 0 \right). \quad (6.43)$$

For these α -couplings we get $\det(A) = 14/d - 2$; therefore, the matrix A is invertible for $d < 7$. However, using (6.20), y_1^2 we see that is negative, and, since $\Lambda_1 = f^2 > 0$, the proper critical point does not exist. Apart from the equator, there is another critical point, which has $y_1 = 0$ and $y_2 \neq 0$ and corresponds to a power-law behaviour with exponent $p = d/(d+2)$. This critical point is an attractor and the equator is a repeller. Thus, an S2-brane reduced to four dimensions corresponds to a solution interpolating between the equator and the attracting critical point. This is similar to the behaviour of the solution found in [83], which is the fluxless limit of a reduced S2-brane [91]. Indeed, the attracting power-law solution is the same with or without flux. Examples of interpolating solutions, projected on the (x_1, x_2) -plane, are shown in figure 6.3, in the case of $d = 2$. One can see that they indeed interpolate between the equator and the attracting critical point, which, according to (6.26), has the coordinates $(x_1, x_2) = (\sqrt{2/3}, 0)$. For $d = 7$, there is a possibility of a de Sitter solution, since $\det(A) = 0$, see (6.37). However, it does not exist because y_1^2 is negative.

6.4.3 Triple exponential potential, one scalar

This example is the simplest case where the y -variables are not all independent, and this subsection serves as an illustration. The potential is described in terms of three dilaton couplings α_1 , α_2 , and α_3 . For simplicity, we take $\Lambda_i > 0$; the case with negative Λ_i can be analysed in a similar way. We can choose $\alpha_3 > 0$. Since $R = 1$, we have two independent y 's, leaving one relation, which reads

$$(\Lambda_2)^{\alpha_1 - \alpha_3} (y_2^2)^{\alpha_3 - \alpha_1} = (\Lambda_1)^{\alpha_2 - \alpha_3} (\Lambda_3)^{\alpha_1 - \alpha_2} (y_1^2)^{\alpha_3 - \alpha_2} (y_3^2)^{\alpha_2 - \alpha_1}. \quad (6.44)$$

The analysis of critical points is analogous to the previous case, except for the extra feature of the relation above. There are three kinds of critical points (for the moment we leave aside the y -dependence)

$$\begin{aligned}
 (i) \quad & y_i = 0, \quad x^2 = 1, \\
 (ii) \quad & y_i = y_j = 0, \quad y_k = \sqrt{1 - \frac{\alpha_k^2}{3}}, \quad x = \frac{\alpha_k}{\sqrt{3}}, \quad i, j, k \text{ different} \\
 (iii) \quad & x = 0.
 \end{aligned} \tag{6.45}$$

A necessary condition for its existence is $\alpha_k^2 < 3$. However, this is not sufficient, since (6.44) only allows certain y 's to be non-zero while the others are zero. For instance, with $\alpha_3 > \alpha_2 > \alpha_1$, having $y_1 = 0$ or $y_3 = 0$ implies $y_2 = 0$.

The third type of critical point is a de Sitter solution given by the following equations:

$$\alpha_1 y_1^2 + \alpha_2 y_2^2 + \alpha_3 y_3^2 = 0, \quad y_1^2 + y_2^2 + y_3^2 = 1, \tag{6.46}$$

which can be rewritten as

$$\frac{\alpha_3 - \alpha_1}{\alpha_3} y_1^2 + \frac{\alpha_3 - \alpha_2}{\alpha_3} y_2^2 = 1. \tag{6.47}$$

This defines an ellipse for $\alpha_3 > \alpha_1, \alpha_2$. When substituting y_3 , (6.44) also gives a curve in the (y_1, y_2) -plane, and the critical point is given as the intersection between these two curves.⁶ For example, for $(\alpha_1, \alpha_2, \alpha_3) = (-1/2, 1/2, 3/2)$ and $\Lambda_i = 1$, the de Sitter critical point becomes $(y_1 = 0.78, y_2 = 0.52, y_3 = 0.34)$. Figure 6.4 shows the time-development of an interpolating solution for this case. One can see that the late-time behaviour indeed corresponds to the de Sitter critical point above.

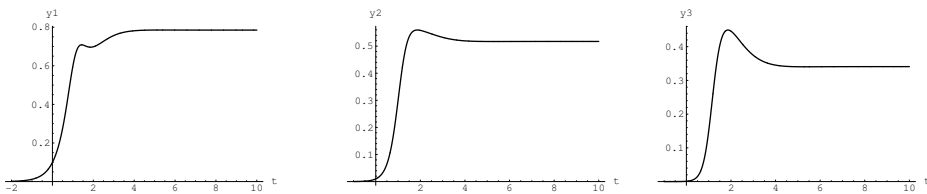


Figure 6.4: The plots show $y_1(t)$, $y_2(t)$ and $y_3(t)$, respectively. As t increases, they tend towards the de Sitter critical point.

6.5 Multi-exponential potentials from group manifolds

In this section we will consider specific cases that can be obtained by reducing pure gravity in seven dimensions over a three-dimensional group manifold. See appendix C for a basic

⁶However, it is only possible to give algebraic expressions of the solution for special values of the dilaton couplings.

definition of group manifolds. Since pure gravity in 7D can be embedded in 11D, the solutions have an M-theory origin. We will focus on the triple-exponential case.

Double exponential potentials can be obtained for certain truncations of reductions over type VIII and IX group manifolds [95]. This is equivalent to a trivial reduction over a circle followed by a reduction over a maximally symmetric 2D space with flux. The resulting potential is given by (6.40), with $d = 2$, and interpolating solutions correspond to reductions of S2-branes from six dimensions.

A triple exponential potential can be obtained from type VI₀ and VII₀ group manifolds and the result is [95]

$$V = \frac{1}{8} e^{-\sqrt{3}\varphi} (e^\phi \pm e^{-\phi})^2, \quad (6.48)$$

where the plus sign occurs for type VI₀ and the minus sign for type VII₀. We therefore have an example with $m = 3$ and $N = 2$, and the three dilaton couplings are

$$\vec{\alpha}_1 = (\sqrt{3}, 2), \quad \vec{\alpha}_2 = (\sqrt{3}, -2), \quad \vec{\alpha}_3 = (\sqrt{3}, 0). \quad (6.49)$$

Note that only two of these are independent, hence this case falls into the $R < m$ class, and, more interestingly, we find the convex combination $\frac{1}{2}\vec{\alpha}_1 + \frac{1}{2}\vec{\alpha}_2 = \vec{\alpha}_3$. Therefore, a proper critical point with power-law behaviour is possible. The fact that we have linearly dependent $\vec{\alpha}_i$ -vectors ($R < m$) is actually the case for most Bianchi class A types. For the present example, there will be two independent y -variables plus the relation $y_3 = \pm 2y_1y_2$, but only y_1 and y_2 are needed.

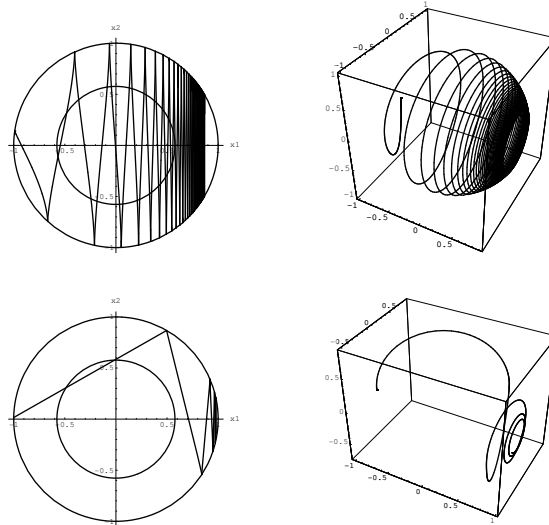


Figure 6.5: Type VII₀. On the left-hand-side are shown the projection of two interpolating solutions on the (x_1, x_2) -plane. On the right-hand-side, the curves are shown on the 2-sphere defined by the Friedmann equation; the vertical axis is given by $y_1 - y_2$. The fact that the curves do not reach the attractor is due to the finite computation time.

For the sake of illustration, $y_1 \pm y_2$ can be used as a variable, such that any solution will be given by points or curves on a 2-sphere (the upper half in the case of the plus sign, since the y 's are positive). Interestingly, the dilaton couplings are such that most of the critical points from the previous section do not exist. In fact, for type VI₀, we are just left with the equator solutions and for type VII₀ we have the equator and an infinite set of proper solutions:

$$\left. \begin{aligned} x^2 = 1, & & y_1 = y_2 = 0 & & \text{type VI}_0, \\ x^2 = 1, & & y_1 = y_2 = 0 & & \\ (x_1, x_2) = (1, 0), & & y_1 = y_2 & & \text{type VII}_0. \end{aligned} \right\} \quad (6.50)$$

By studying the derivatives of the coordinates, it can be shown that the following points are attractors

$$\left. \begin{aligned} (x_1, x_2) = (1, 0) & & y_1 = y_2 = 0 & & \text{type VI}_0, \\ (x_1, x_2) = (1, 0) & & y_1 = y_2 & & \text{type VII}_0. \end{aligned} \right\} \quad (6.51)$$

Thus, the latter is not unique since the y_i -values are arbitrary. The solution corresponds to (6.32), which is possible because of the convex combination: $\vec{\alpha}_3 = (\vec{\alpha}_1 + \vec{\alpha}_2)/2$. In both cases any interpolating solution will end in the point (1, 0, 0) on the 2-sphere. In the VII₀ case, the y -value will be determined by the initial conditions. The sign of \dot{x}_1 is always positive. When projected on the (x_1, x_2) -plane, any curve will therefore move from left to right.

A stability analysis leads to the result that only the part of the equator with $x_1 < -1/7$ is repelling. Thus, any interpolating solution can start on this part and will end in (1, 0, 0).

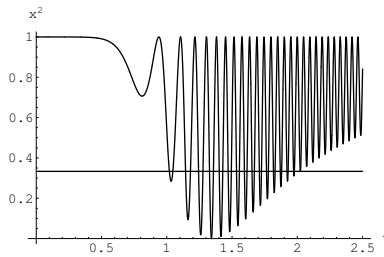


Figure 6.6: Type VII₀. An example of a (t, x^2) -plot with $n < 1$.

A couple of typical curves for interpolating solutions with different initial conditions are depicted on figure 6.5, for type VII₀. In this case, any curve will spiral around the 2-sphere towards the attractor. The projection on the (x_1, x_2) -plane produces a curve which bounces off the boundary of the unit circle. The inner disc, corresponding to $x^2 < 1/3$, yields phases of accelerated expansion. Depending on the initial conditions, the number of such phases can be as high or low as desired. For the two cases on figure 6.5, the numbers are 16 and 1, respectively. Even with a large number of accelerating phases, the number of e-foldings is of order 1; therefore, these models are not well suited for inflation. The numerical solutions use $t = \ln(a)$ as time parameter. The number of e-foldings is given by

$$n = \ln\left(\frac{a(\tau_2)}{a(\tau_1)}\right) = \ln\left(\frac{e^{t_2}}{e^{t_1}}\right) = \Delta t, \quad (6.52)$$

and its order of magnitude can easily be read off from a (t, x^2) -plot as the sum of the t -intervals where $x^2 < 1/3$. An example is given in figure 6.6.

For type VI₀, the situation is slightly different, since $y_1 + y_2$ is always positive; this confines the curves to the upper half of the 2-sphere. On figure 6.7, the curves still move towards the attractor in an oscillatory manner, but now without crossing the equator (though they can get arbitrarily close). For this case, there can only be one or no phase of accelerated expansion.

The interpolating solutions above correspond to reductions of exotic S2-branes in five dimensions, or equivalently, exotic S($D - 3$)-branes in D dimensions. However, the solutions were found numerically, and we have not been able to obtain exact expressions for these exotic S-branes.

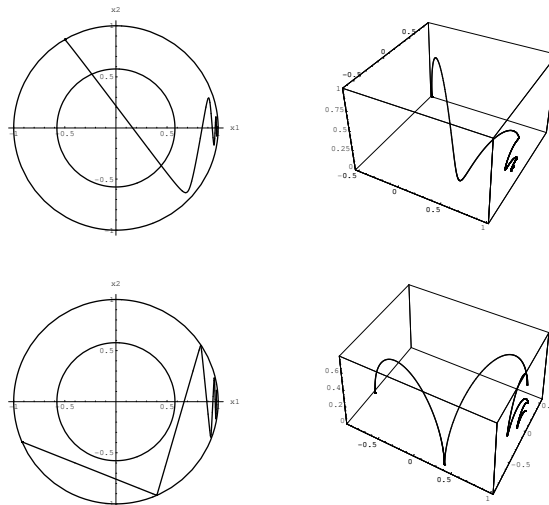


Figure 6.7: Type VI₀. On the left-hand-side are shown the projections of two interpolating solutions on the (x_1, x_2) -plane. On the right-hand-side, the curves are shown on the 2-sphere defined by the Friedmann equation; the vertical axis is given by $y_1 + y_2$.

6.6 Discussion

In this chapter we have considered cosmological models for an arbitrary number of scalars with arbitrary multi-exponential potentials. Using a special set of variables, the equations were written as autonomous dynamical systems, and this allowed us to determine the critical points in complete generality. We found that the nature of these critical points depends strongly on the rank R of the matrix α_{iI} . The rank also determines the number of decoupled scalars.

In the case $R = m$, both the proper and non-proper critical points are power-law solutions, and there are no de Sitter solutions. In the $R < m$ case the opposite behaviour was found. Proper power-law solutions are only possible in special cases, where the $\vec{\alpha}_i$ -vectors are linearly dependent in a specific way, but the de Sitter solutions are very generic. For the non-proper

solutions, this depends on whether the “truncated” potential has $R = m$ or $R < m$. We also found a new property of these systems, namely the possibility of proper critical points that are not unique. A special case was realized in section 5, where we have an infinite set of these.

It should be emphasized that the non-proper critical points are as important as the proper ones for understanding the interpolating solutions, even though they have not often been considered in the literature. In this respect, using the techniques of autonomous systems is more fruitful than simply looking for power-law solutions to the equations of motion.

It should be pointed out that in our solutions the scalars generically have run-away behaviour. The only exceptions are the de Sitter critical points, since these correspond to extrema of the potential and accordingly stabilize the values of the scalars. This is important in the context of spontaneous decompactification [134] or stabilization of dilaton and volume moduli [33]

In section 4 and 5, we provided several examples of double and triple exponential potentials. We presented the critical points and illustrated the interpolating solutions using numerical calculations. In particular, we found examples with an arbitrarily high number of phases of accelerated expansion. However, the number of e-foldings turned out to be of order one, so these models do not seem to be relevant for inflation. They might, however, be relevant for present-day acceleration and they might help solve the cosmic coincidence problem.

The numerical solutions found in section 5 for the systems obtained from reductions over group manifolds of type VI_0 and type VII_0 correspond to the reduction of exotic S2-branes in five dimensions. The two solutions belong to a set of three different solutions that can be obtained via twisted circle reductions. The third solution can be obtained from a reduction over the type II group manifold and corresponds to the reduction of a fluxless S2-brane. The existence of three classes of S-branes is similar to the cases of 7-branes in ten dimensions [42] and the non-extremal D-instantons we studied in chapter 3, and it is reminiscent of the global $SL(2, \mathbb{R})$ -symmetry of the higher dimensional theory. It would be interesting to see whether it would be possible to find exact solutions for the exotic S-branes.

Recently, an elegant framework for arbitrary potentials has been developed, where the solutions correspond to geodesics in an augmented target space [135]. One of the key ingredients is the importance of systems whose late-time behaviour is governed by single exponential potentials [94]. In our analysis, these solutions asymptote to the special class of non-proper critical points where all y 's but one vanish. However, we have shown that multi-exponential potentials have solutions, where the asymptotics cannot be governed by a single term in the potential. Specific examples are given by the cases of assisted inflation [108] and generalized assisted inflation [122], where each term in the potential contributes.

Comments on some possible extensions of this work would be in order. First of all, we have only considered flat universes, and it is certainly possible to extend this formalism to the spatially curved cases.

Secondly, we could also add matter, in the form of a barotropic fluid. This could play a rôle in solving the cosmic coincidence problem. The authors of [107] showed that a system with one scalar and a barotropic fluid can have attractor solutions that are neither scalar-field dominated nor matter dominated, but both at the same time. These are the so-called *scaling solutions* where dark energy and matter coexist. This may lead to a dynamical solution to the cosmic coincidence problem. In other words, a scaling solution dynamically explains why dark energy and matter have comparable energy densities, in the present universe. However, in the one-scalar system

studied in that paper, the de Sitter attractor and the scaling attractor are mutually exclusive. Given a dilaton coupling, only one can exist. Although it is not known whether the universe will be eternally de Sitter, some string theory based scenarios rely upon stable de Sitter vacua that the universe ‘tunnels’ out of by quantum mechanical effects. Hence, it could be interesting to have a combined scaling-de Sitter attractor. By having a more complex system than the one-scalar Lagrangian, one might obtain a compromise between a pure de Sitter and a scaling solution. In [106] and [122], scalars were added to make systems with assisted and generalized assisted inflation, respectively. In [136], spatial curvature was added in the one-scalar case. The potentials we have considered here, however, allow for new de Sitter attractors. They also allow for oscillatory behavior; i.e. some of the solutions are periodic in time. An oscillatory universe might also explain cosmic coincidence. The chances of living in a period where dark energy and matter coexist are greater in a universe that forever oscillates between dark energy and matter domination. In this same spirit, we hope to extend the search for scaling solutions to the most general exponential potential with spatial curvature and a barotropic fluid and report on it in a future publication.

Thirdly, we could consider non-flat scalar manifolds. Finally, we could consider other specific numerical examples with other values of m and N and special dilaton couplings which arise from dimensional reductions of string/M-theory.

This concludes the second part of this thesis, which covered the topic of cosmological solutions. Both this and the previous part dealt with scalar-gravity solutions that depend on one parameter. D-instantons depend on one spatial direction, whereas cosmologies depend on time only. Both types of solution have the generic property of interpolating between ‘trivial’ configurations: The wormhole solution interpolates between two regions with flat spacetime and constant fields, and the cosmologies interpolate between power-law and/or de Sitter spacetimes. In the next and final chapter of this thesis, we will establish links between D-instantons and cosmologies. We will actually show two ways in which these objects can correspond to each other. First, we will see that they can sometimes be related to each other via Wick rotations. Then, we will show that by means of a paradigm shift, both types of solutions can be regarded as trajectories of a particle in a fictitious spacetime, a target space parametrized by the scalars in the Lagrangian.